In Situ Generation of HCN for Mass Spectrometric Studies

Silvi A. Chacko, Ian H. Krouse, Loubna A. Hammad, and Paul G. Wenthold
Department of Chemistry, Purdue University, West Lafayette, Indiana, USA

Hydrogen cyanide (HCN) for use in ion preparation can be generated in the gas phase by the neutral–neutral reaction of trimethylsilyl cyanide (Me_3SiCN) and water in a flowing afterglow mass spectrometer. We demonstrate that the approach can be used to generate a wide range of HCN solvated ions such as $F^-(HCN)$, $Cl^-(HCN)$, $CN^-(HCN)$, $PhNO_2^-(HCN)$, $Me_3SiO^-(HCN)$,and $PhSiF_4^-(HCN)$, many of which are otherwise difficult to generate. The bond dissociation energy of $CN^-(HCN)$, generated by using this approach, has been measured by using energy-resolved collision-induced issociation (CID) to be 0.87 ± 0.07 eV. (J Am Soc Mass Spectrom 2006, 17, 51–55) © 2005 American Society for Mass Spectrometry

Studies of hydrogen-bonding interactions between gaseous anions and neutral molecules [1] have provided a greater perspective to the understanding of solvation of ions [2, 3] in both the condensed phase and the gas phase. Whereas solvated halide [4, 5] and alkoxide [6] ions are readily examined, clusters of cyanide are especially of interest because CN^- is a pseudohalide with an ambidentate nature. Moreover, the conjugate acid, HCN, is a weak acid (ΔH_{acid} = 350.9 ± 0.2 kcal/mol) [7] with extensive positive charge character on the hydrogen, making it an attractive hydrogen-bonding moiety in the gas phase [8]. Recently, HCN has gained much interest as it has been found to be a tracer for young stellar objects, and it has been detected in the atmosphere of Titan [9].

An important challenge in carrying out studies involving cyanide or hydrogen cyanide is in the safe generation of the reagents. Because of its toxicity, HCN is rarely used directly as a reagent gas. Previous studies by Larson and McMahon [8] and Meot-Ner and coworkers [10] have used the solution phase reaction of KCN and acids (HCl or H_2SO_4) to produce HCN, which was directly added to the mass spectrometer. Subsequently, ion-exchange equilibria [8] and van't Hoff measurements [10] were used to determine anion-neutral binding energies of CN^- and HCN containing clusters. Recent studies have utilized the reaction of CH_4 and NH_3 with Pt catalyst to generate HCN in a molecular beam apparatus [11].

In this work, we describe a simple in situ approach for generation of HCN for ion clustering studies. Hydrogen cyanide is formed by the neutral–neutral reaction of trimethylsilyl cyanide, Me_3SiCN, with water in a flowing afterglow reactor. We demonstrate that the approach can be used to generate a wide range of HCN solvated ions and report energy-resolved CID studies of the $HC_2N_2^-$ ion formed. From these CID studies, we report a direct measurement of the $[CN—HCN]^-$ bond dissociation energy. Throughout this paper, $HC_2N_2^-$ refers to the *m/z* 53 species that has been observed and characterized. However, this notation does not indicate a specific ion structure. The structures of the $HC_2N_2^-$ isomers are addressed computationally at the end of this study.

Experimental

All experiments were carried out in a flowing afterglow triple quadrupole mass spectrometer that has been previously described [12, 13]. Fluoride was prepared by 70 eV electron ionization of neutral fluorine gas (5% in He, Spectra Gases Inc., Branchburg, NJ) and carried by helium buffer gas (0.400 torr, flow (He) = 190 STP cm^3/s) through the flow tube where it was allowed to react with neutral reagent vapors, either added through micrometering valves or generated by neutral-neutral reactions. The phenyltetrafluorosiliconate ion, $C_6H_5SiF_4^-$ was generated by termolecular addition of fluoride with $PhSiF_3$. Chloride and trimethylsiloxide ions were formed by the reaction of OH^- with chloroethane and hexamethyldisiloxane, $(CH_3)_3SiOSi(CH_3)_3$, respectively. The nitrobenzene anion, $PhNO_2^-$, was formed by direct electron attachment in the high-pressure source. Ions were collisionally cooled to ca. 300 K within the helium buffer.

Energy resolved mass spectrometry experiments are carried out by selecting ions with the desired mass-to-

Published online December 15, 2005
Address reprint requests to Dr. P. G. Wenthold, Department of Chemistry, Purdue University, 560 Oval Drive, West Lafayette, IN 47907-2084, USA. E-mail: pgw@purdue.edu

1044-0305/06/$32.00
doi:10.1016/j.jasms.2005.08.018

Received July 25, 2005
Revised August 27, 2005
Accepted August 27, 2005

charge ratio by using the first quadrupole (Q1) and injecting them into the second quadrupole (q2, radio frequency only) where they undergo collision-induced dissociation (CID) with neon gas. Product ions are mass analyzed with the third quadrupole (Q3) and detected with a channeltron electron multiplier. The collision energy of the primary ion in q2 was varied and fragment ion intensities were monitored as a function of q2 rod offset voltage to yield energy-resolved mass spectra. The kinetic energy distribution of the ions was determined by retarding potential analysis.

CID cross-sections, σ, were calculated using $I/I_o = \sigma N l$, where I and I_o are the intensities of the product and reactant ions, respectively, N is the number density of the target, and l is the effective collision path length. The effective path length was measured to be 24 ± 4 cm [13] by using the reaction of $Ar^+ + D_2 \rightarrow ArD^+ + D$ [14]. Cross sections are measured at several different pressures from 0.075 to 0.200 mTorr, and extrapolated to zero pressure, single collision conditions.

Data Analysis

Collision-induced dissociation (CID) cross sections were modeled with the expression shown in (eq 1) [15, 16] where E is the center-of-mass collision energy of the reactant ion, g_i is the fraction of the ions with internal energy E_i, E_0 is the threshold energy for dissociation, n is a parameter that reflects the energy deposition in the collision [17], and σ_0 is a scaling factor. Also convoluted into the fit were the ion kinetic energy distributions, approximated as a Gaussian function with a 1.5 eV (laboratory frame) full-width at half-maximum, and a Doppler broadening function to account for motion of the target gas. The factor P_i is the probability for ion dissociation, calculated from RRKM theory.

$$\sigma(E) = \sigma_0 \sum_i P_i g_i (E + E_i - E_0)^n / E \quad (1)$$

The data are modeled by adjusting the parameters to correspond with the steeply rising portion of the appearance curve directly above the onset. Data analysis and modeling of the cross sections were carried out using the CRUNCH 4D program developed by Armentrout and coworkers [14–16, 18, 19]. Modeled threshold energies, E_0, are 0 K ΔE values converted to 298 K bond dissociation enthalpies by using the integrated heat capacities of reactants and products. Uncertainties in enthalpy values were calculated by statistical combination of the uncertainty in the absolute energy scale for the experiment, (0.15 eV laboratory frame) and the standard deviation of values obtained from replicate experimental trials.

Computational Details

Geometries, absolute energies, vibrational frequencies, and enthalpies for isomers of $HC_2N_2^-$ were calculated using density functional theory (B3LYP [20], perturbation theory (MP2 [21, 22] and Complete Basis Set methods (CBS [23]).

Materials

Trimethylsilyl cyanide, Me_3SiCN, and trifluorophenylsilane were distilled under atmospheric conditions before use. Nitrobenzene and chloroethane were used as received. All reagents were purchased from commercial sources. Liquid samples were degassed by successive freeze-pump-thaw cycles before use. Helium was purified via a liquid nitrogen trap containing molecular sieves. Gas purities are as follows: He (99.995%), F_2 (5% in helium), CH_4 (99%), N_2O (99%), Ne (99%). CAUTION: As with any source of HCN, trimethylsilyl cyanide should be handled with proper safety precautions, as described by the MSDS.

Results and Discussion

The flowing afterglow [12] is a versatile reaction vessel commonly used as an ion source in mass spectrometry. However, recognizing that flow reactors are not limited to ionic systems [12, 24–26], we reasoned that neutral–neutral reactions in the flowing afterglow could be used to generate gaseous samples of reagents generally too corrosive or hazardous to be handled using standard techniques. Although neutral–neutral reactions are generally not as fast as ion/molecule reactions, concentrations of neutral reagents are significantly higher than those for ions and, therefore, sufficient amounts of products can be obtained. This process is demonstrated by the reaction of Me_3SiCN and water to generate neutral species, Me_3SiOH and HCN (eq 2) in the flow tube.

$$(CH_3)_3SiCN + H_2O \rightarrow HCN + (CH_3)_3SiOH \quad (2)$$

Silanols can be prepared in the condensed phase by the hydrolysis of silane derivatives in the presence of acid acceptors or bases such as ammonium bicarbonate or aniline [27]. Similarly, De Sarlo and coworkers have shown that Me_3SiOH can be formed in the reaction of Me_3SiCNO with water [28]. We observe the formation of HCN when both Me_3SiCN and water vapor are added to the flowing afterglow mass spectrometer. The formation of HCN is indicated by the appearance of ionic clusters. Upon chemical ionization with F^-, cyanotrimethylsilane undergoes substitution to form CN^-. With only Me_3SiCN, the products observed under typical conditions include CN^- (99%) and the CN^- adduct of the silane, $CN^-(Me_3SiCN)$ (1%). The additional products observed when water is added into the flow tube include ionic products corresponding to the HCN adducts $CN^-(HCN)_n$ (n = 1–3) (~30%), $F^-(HCN)$ (~5%), Me_3SiO^- (~5%), $CN^-(Me_3SiCN)$ (~10%), $CN^-(Me_3SiOH)$ (~20%), and CN^- (~30%). This indicates the formation of neutral products HCN

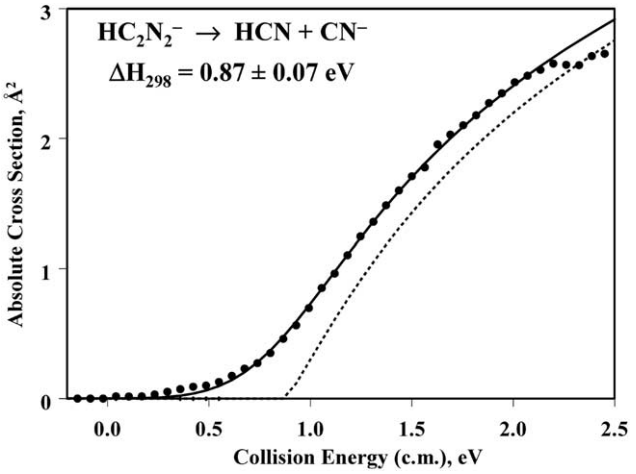

Figure 1. Cross-sections for CN^- formation from collision-induced dissociation of $HC_2N_2^-$ (*m/z* 53) with Ne target as a function of translational energy (center-of-mass). The solid line is the model appearance curve calculated using eq 1, and the broken line represents the unconvoluted function.

and Me_3SiOH. The fact that the HCN clusters and Me_3SiOH clusters are only observed in the presence of both Me_3SiCN and water suggests that these neutral products are formed by the neutral–neutral reaction. In principle, the acid does not need to be water, and we obtained similar results by using HF. However, water is a more convenient and less corrosive reagent.

To demonstrate the general applicability of this preparation, we have used it to generate HCN clusters of a wide range of ions, including F^-, Cl^-, Me_3SiO^-, $PhSiF_4^-$, and $PhNO_2^{\cdot-}$. Although many HCN cluster ions can be readily generated by the reaction of CN^- with acid, this approach can also be used with ions that do not have convenient conjugate acids. For example, whereas trimethylsilanol (Me_3SiOH) is not a readily available reagent, the cluster of $HCN(Me_3SiO^-)$ can be generated by reaction of Me_3SiO^- and HCN. Similarly, we are able to generate HCN clusters of $PhSiF_4^-$ and $PhNO_2^{\cdot-}$ ions that cannot be conveniently prepared by alternate methods. The observation that HCN clusters can be formed with $PhSiF_4^-$ and $PhNO_2^{\cdot-}$ is also evidence that HCN is being formed by the reaction of trimethylsilyl cyanide and water, and not by the reaction of trimethylsilyl cyanide and hydrated ions, because these ions are not efficiently hydrated in the presence of water.

As noted, the approach also provides a convenient synthesis of the CN^-(HCN) cluster ion. The reactivity of $HC_2N_2^-$ (*m/z* 53) was studied by ion/molecule reactions. In the flowing afterglow, $HC_2N_2^-$ undergoes condensation reactions with CO_2 and CS_2 and forms a cluster ion with NO (*m/z* 83). A single H/D exchange occurs on reaction with CH_3OD, indicative of the presence of a hydrogen atom. This reaction is somewhat surprising considering the large difference in the acidities of methanol and HCN [29], and likely occurs as a result of cooperativity of the HCN solvent molecule in the reaction complex. CID of $HC_2N_2^-$ (*m/z* 53) gives exclusive formation of CN^- (*m/z* 26) indicating that the $HC_2N_2^-$ species is an HCN cluster of cyanide, CN^-(HCN).

The bond dissociation energy of CN^-(HCN) was determined by energy-resolved collision-induced dissociation. A plot of the cross sections as a function of center-of-mass collision energy is shown in Figure 1. The 298 K enthalpy for CN^- loss obtained from modeling of the cross sections is 0.87 ± 0.07 eV for the CN^-(HCN) cluster. For the purposes of modeling, vibrational frequencies and rotational constants were used for the CN^-—HCN isomer, which is the lowest energy structure (see below). However, modeling the data by assuming a NC^-—HCN structure gave the same result. The measured value is in good agreement with previously reported values of 0.94 ± 0.15 eV [8] and 0.90 ± 0.04 eV [10], obtained by using ion cyclotron resonance and high-pressure mass spectrometry, respectively.

Because CN^- is an ambidentate nucleophile, it may bind to the hydrogen either at the carbon site or the nitrogen site in a cluster. Previous SCF computational studies by Cybulski and Scheiner indicate that the CN^-—HCN isomer is more stable than the NC^-—HCN isomer by ca. 0.6 kcal/mol [30]. Similarly, SCF and MP2 calculations reported by Meot-Ner and coworkers [10] predict the nitrogen-bonded geometry to be more stable by 1 to 2 kcal/mol, in agreement with the results obtained by Cybulski and Scheiner [30]. Moreover, it is also in agreement with the calculations of Jorgensen et al. [31], which found that the N-bonded geometry is favored in hydrated CN^-. Meot-Ner et al. [10] interpret the similarity between the energies of the two isomers as an indication of little anisotropy in the CN^- ion.

In the present work, we have studied the CN^-(HCN) clusters using various computational methods, including B3LYP, MP2 and CBS. Four isomers of $HC_2N_2^-$ were considered: NC^-—HCN, CN^-—HCN, NC^-—HNC and CN^-—HNC. The structures NC^-—HCN and CN^-—HCN are adducts of HCN, whereas NC^-—HNC

Table 1. Relative enthalpies at various levels of theory for $HC_2N_2^-$ isomers (kcal/mol)[a]

Method	NC^-—HCN	CN^-—HCN	CN^-—HNC
B3LYP/6-31+G*	0.6	0.0	6.2
B3LYP/6-311++G**	0.9	0.0	4.7
B3LYP/6-311++G** (3df,3pd)	0.8	0.0	4.7
B3LYP/aug-cc-pVDZ	1.0	0.0	3.5
B3LYP/aug-cc-pVTZ	0.9	0.0	4.7
CBS-APNO	1.2	0.0	5.9
G2	1.4	0.0	6.3
G2MP2	1.5	0.0	5.8
G3	1.2	0.0	6.4
G3MP2	1.4	0.0	6.2
MP2/aug-cc-pVDZ	0.6	0.0	6.1
MP2/6-31 + G*	0.4	0.0	9.7

[a]298 K enthalpies relative to CN^-—HCN.

Table 2. Computed enthalpies for the dissociation of stable $HC_2N_2^-$ isomers[a] at various levels of theory

Method/Basis Set	NC^-—HCN[b] BDE (eV)	CN^-—HCN[b] BDE (eV)	CN^-—HCN[c] BDE (eV)	CN^-—HNC[c] BDE (eV)
B3LYP				
6–31+G*	0.89	0.92	1.55	1.28
6–311++G**	0.89	0.93	1.54	1.34
6–311++G** (3df,3pd)	0.90	0.93	1.53	1.33
aug-ccVDZ	0.94	0.98	1.56	1.40
aug-ccVTZ	0.90	0.93	1.53	1.33
MP2				
6-31 + G*	0.83	0.85	1.68	1.26
aug-cc-pVDZ	0.91	0.94	1.71	1.45
Extrapolation Methods				
CBS-APNO	0.90	0.95	1.58	1.32
G2	0.84	0.90	1.53	1.26
G2MP2	0.84	0.91	1.51	1.26
G3	0.86	0.91	1.54	1.26
G3MP2	0.83	0.89	1.51	1.24
Experimental				
This Work		0.87 ± 0.07		
		0.94 ± 0.15 [8]		
		0.90 ± 0.15 [10]		

[a]Isomer NC^-—HNC is not a stable structure, and collapses to CN^-—HCN.
[b]Formation of HCN + CN^-
[c]Formation of HNC + CN^-

and CN^-—HNC are nominally adducts of isohydrocyanic acid, HNC. However, regardless of the starting geometry, it is found that NC^-—HNC always optimizes to a NCH—$^-$NC structure. Moreover, a fixed geometry with a structure NC^-—HNC is calculated to be unstable and ca. 8 kcal/mol higher in energy than CN^-—HCN. Therefore, there are likely only three stable geometries of the cyanide cluster. Relative energies of the $HC_2N_2^-$ isomers and the corresponding DH_{298} bond dissociation energies are shown Tables 1 and 2. At all levels of theory, the CN^-—HCN ion is the lowest energy structure, but only slightly lower in energy than NC^-—HCN. Moreover, the predicted BDEs for CN^-—HCN and NC^-—HCN agree to within 0.05 eV. Therefore, the isomers are sufficiently close in energy and have similar BDEs such that they cannot be distinguished experimentally. The CN^-—HNC isomer is predicted to be ca. 6 kcal/mol higher in energy than the CN^-—HCN structure, and has a calculated BDE of ca. 1.4–1.5 eV (Table 2), much higher than the measured BDE of 0.87 eV. This indicates that the reaction of $(CH_3)_3SiCN$ with water likely forms HCN and not HNC. The formation of HCN is not surprising considering the large energy difference between the two isomers [32].

Conclusions

The results from this work demonstrate a safe, easy, noncorrosive and environment-friendly generation of HCN in the gas-phase for mass spectrometric studies. An advantage to the present approach is that it can be used for studying various ion clusters that are not easily accessible by reactions of CN^- ion. The bond dissociation energy for CN^-(HCN) was measured to be 0.87 ± 0.07 eV using energy-resolved CID measurements, in good agreement with previously reported values and thermochemical predictions. Theoretical calculations predict the lowest energy structure of $HC_2N_2^-$ to be CN^-—HCN, although NC^-—HCN is only slightly higher in energy and these structures are not experimentally distinguishable.

Acknowledgments

This work was supported by the National Science Foundation (grant no. CHE-0137627).

References

1. Takashima, K.; Riveros, J. M. Gas-Phase Solvated Negative Ions. *Mass Spectrom. Rev.* **1998,** *17,* 409–430.
2. Krestov, G. A., *Thermodynamics of Solvation: Solution and Dissolution, Ions and Solvents, Structure and Energetics*. Ellis Horwood: New York, 1991.
3. Dyumaev, K. M.; Korolev, B. A. The Influence of Solvation on Acid-Base Properties in Various Media. *Russ. Chem. Rev.* **1980,** 49, 1021–1032.
4. Larson, J. W.; McMahon, T. B. Strong Hydrogen Bonding in Gas-Phase Anions. An Ion Cyclotron Resonance Determination of Fluoride Binding Energetics to Brønsted Acids from Gas-Phase Fluoride Exchange Equilibria Measurements. *J. Am. Chem. Soc.* **1983,** *105,* 2944–2950.
5. Larson, J. W.; McMahon, T. B. Hydrogen Bonding in Gas-Phase Anions. An Experimental Investigation of the Interaction between Chloride Ion and Brønsted Acids from Ion Cyclotron Resonance Chloride Exchange Equilibria. *J. Am. Chem. Soc.* **1984,** *106,* 517–521.
6. Caldwell, G.; Rozeboom, M. D.; Kiplinger, J. P.; Bartmess, J. E. Anion–Alcohol Hydrogen Bond Strengths in the Gas-Phase. *J. Am. Chem. Soc.* **1984,** *106,* 4660–4667.
7. Bradforth, S. E.; Kim, E. H.; Arnold, D. W.; Neumark, D. M. Photoelectron Spectroscopy of CN^-, NCO^-, and NCS^-. *J. Chem. Phys.* **1998,** *98,* 800–810.
8. Larson, J. W.; McMahon, T. B. Hydrogen Bonding in Gas-Phase Anions. The Energetics of Interaction Between Cyanide Ion and Brønsted Acids Determined from Ion Cyclotron Resonance Cyanide Exchange Equilibria. *J. Am. Chem. Soc.* **1987,** *109,* 6230–6236.
9. Yun, J. L.; Moreira, M. C.; Afonso, J. M.; Clemens, D. P. HCN in Cloud Cores: A Good Tracer of Class 0 Young Stellar Objects. *Astro. J.* **1999,** *118,* 990–996.

10. Meot-Ner, M.; Cybulski, S. M.; Scheiner, S.; Leibman, J. F. Is CN^- Significantly Anisotropic? Comparison of CN^- vs Cl^-: Clustering with HCN and Condensed-Phase Thermochemistry. *J. Phys. Chem.* **1988,** *92,* 2738–2745.
11. Horn, R.; Mestl, G.; Thiede, M.; Jentoft, F. C.; Schmidt, P. M.; Bewersdorf, M.; Weber, R.; Schlögl, R. Gas-Phase Contributions to the Catalytic Formation of HCN from CH_4 and NH_3 Over Pt: An in Situ Study by Molecular Beam Mass Spectrometry with Threshold Ionization. *Phys. Chem. Chem. Phys.* **2004,** *6,* 4514–4521.
12. Graul, S. T.; Squires, R. R. Advances in Flow Reactor Techniques for the Study of Gas-Phase Ion Chemistry. *Mass Spectrom. Rev.* **1988,** *7,* 263–358.
13. Marinelli, P. J.; Paulino, J. A.; Sunderlin, L. S.; Wenthold, P. G.; Poutsma, J. C.; Squires, R. R. A Tandem Selected Ion Flow Tube Triple Quadrupole Instrument. *Int. J. Mass Spectrom. Ion Processes* **1994,** *130,* 89–105.
14. Ervin, K. M.; Armentrout, P. B. Translational Energy Dependence of $Ar^+ + XY \rightarrow ArX^+ + Y$ (XY = H_2, D_2, HD) from thermal to 30 eV c.m. *J. Chem. Phys.* **1985,** *83,* 166–189.
15. Schultz, R. H.; Crellin, K. C.; Armentrout, P. B. Sequential Bond Energies of Iron Carbonyl $Fe(CO)_x^+$ (x = 1–5): Systematic Effects on Collision-Induced Dissociation Measurements. *J. Am. Chem. Soc.* **1991,** *113,* 8590–8601.
16. Dalleska, N. F.; Honma, K.; Sunderlin, L. S.; Armentrout, P. B. Solvation of Transition Metal Ions by Water. Sequential Binding Energies of $M^+(H_2O)_x$ (x = 1–4) for M = Ti to Cu Determined by Collision-Induced Dissociation. *J. Am. Chem. Soc.* **1994,** *116,* 3519–3528.
17. Muntean, F.; Armentrout, P. B. Guided Ion Beam Study of Collision-Induced Dissociation Dynamics: Integral and Differential Cross Sections. *J. Chem. Phys.* **2001,** *115,* 1213–1228.
18. Rodgers, M. T.; Armentrout, P. B. Statistical Modeling of Competitive Threshold Collision-Induced Dissociation. *J. Chem. Phys.* **1998,** *109,* 1787–1800.
19. Rodgers, M. T.; Ervin, K. M.; Armentrout, P. B. Statistical Modeling of Collision-Induced Dissociation Thresholds. *J. Chem. Phys.* **1997,** *106,* 4499–4508.
20. Becke, A. D. Density-Functional Thermochemistry. III. The Role of Exact Exchange. *J. Chem. Phys.* **1993,** *98,* 5648–5652.
21. Head-Gordon, M.; Pople, J. A.; Frisch, M. J. MP2 Energy Evaluation by Direct Methods. *Chem. Phys. Lett.* **1988,** *153,* 503–506.
22. Sæbø, S.; Almlöf, J. Avoiding the Integral Storage Bottleneck in LCAO Calculations of Electron Correlation. *Chem. Phys. Lett.* **1989,** *154,* 83–89.
23. Ochterski, J. W.; Petersson, G. A.; Montgomery, J. A., Jr. A Complete Basis Set Model Chemistry. V. Extensions to Six or More Heavy Atoms. *J. Chem. Phys.* **1996,** *104,* 2598–2619.
24. Parnis, J. M.; Lafleur, R. D.; Rayner, D. M. Alkane Reactivity with Zr Atoms and Neutral Diatomic ZrO in the Gas Phase. *Chem. Phys. Lett.* **1994,** *218,* 544–550.
25. Lian, L.; Akhtar, F.; Parsons, J. M.; Hackett, P. A.; Rayner, D. M. Gas-Phase Chemical Kinetics of Small Metal Clusters: Development and Characterization of a Fast-Flow Reactor for Neutral Clusters. *Z. Physik D* **1993**, *26*(Suppl.), S168–S170.
26. Weiller, B. H.; Bechthold, P. S.; Parks, E. K.; Pobo, L. G.; Riley, S. J. The Reactions of Iron Clusters with Water. *J. Chem. Phys.* **1989,** *91,* 4714–4727.
27. Cella, J. A.; Carpenter, J. C. Procedure for the Preparation of Silanols. *J. Organomet. Chem.* **1994,** *480,* 23–26.
28. Brandi, A.; De Sarlo, F.; Guarna, A.; Speroni, G. Trimethylsilanecarbonitrile Oxide. *Synthesis* **1982,** *9,* 719–721.
29. DePuy, C. H. Understanding Organic Gas-Phase Anion Molecule Reactions. *J. Org. Chem.* **2002,** *67,* 2393–2401.
30. Cybulski, S. M.; Scheiner, S. Hydrogen Bonding and Proton Transfers Involving Triply Bonded Atoms. HCCH and HCN. *J. Am. Chem. Soc.* **1987,** *109,* 4199–4206.
31. Gao, J.; Garner, D. S.; Jorgensen, W. L. Ab Initio Study of Structures and Binding Energies for Anion–Water Complexes. *J. Am. Chem. Soc.* **1986,** *108,* 4784–4790.
32. Wenthold, P. G. Experimental Enthalpy of Formation of Isonitrile from Collision-Induced Dissociation Threshold Energy Measurements. *J. Phys. Chem. A* **2000,** *104,* 5612–5616.